Journal of Ovonic Research Vol. 17, No.1, January - February 2021, p. 53 - 60

OPTICAL PROPERTIES OF ZnO FILMS PREPARED BY CBD TECHNIQUE

R. A. AL-WARDY[a,*], A. S. ABBAS[b,*], S. I. ABBAS[c,*]

[a]*Clinical laboratory science department, Pharmacy College, Mustansiriyah University, Baghdad, Iraq*

[b]*Department of geophysics, College of remote sensing &geophysics, Al-Karkh University for science, Baghdad, Iraq*

[c]*Medical physics Department, Science College, University of Al-Karkh for science, Baghdad, Iraq*

Thin films of zinc oxide (ZnO) with ammonia solution to 300ml of aqueous solution $\mathrm{Zn(NO_3)_2.6H_2O}$ (0.3M) are created via (CBD) technique on commercial glass substrates with bath temperature $(80 \pm 5)^{\circ}\mathrm{C}$ and annealing temperatures at $(373, 473$ and $573)\mathrm{K}$ at constant time of 1h. The deposited films optical absorbance was defined utilizing SP-3000NANO optima (UV-V is spectrophotometer) and shows that the optical energies gaps for ZnO films increase slightly through a rise in temperature of annealing of the samples at 373K and 473K and register around 3.77eV and 3.78eV respectively. While the energy gap decreases to 3.73eV with increase the annealing temperature at 573K. The wide band gap ZnO has applications of wide array in areas include solar cells, light conductors, chemical sensors and ultraviolet laser diodes.

(Received October 12, 2020; Accepted February 1, 2021)

Keywords: ZnO, CBD method, Thin films, Annealing

1. Introduction

Researchers are attracted by an inorganic material, white powder, low cost and convenient environment of zinc oxide (ZnO) because it is typical candidate for a different devices set to ultra-violet laser from sensors devices [1]. In addition, n-type semi-conductor ZnO was generally 3.37eV direct band gap, high excitation-binding energy (60meV) at room temperature [2-4], high electron mobility $100(cm.V^{-1}sec^{-1})$[1], high visible spectrum clarity, low chemical toxicity and thermal-stability good bio efficiency, and large sufficient being constant below room temperature to make it appropriate for use in device emitting short λ such as diodes light emitting [2]. Currently, (CBD) process has been widely used to obtain ZnO films from aqueous solutions because it is easy to prepare, fast low cost, simple, deposition of large-scale possibilities and does not require a high temperature or vacuum system. In addition, it produces good deposits on suitable substrates by controlled precipitation of solution compounds [4]. Some of the important parameters that affect the properties of ZnO film include solution and process parameters like precursor kind, additives type, solvent type, CBD temperature and time and type of substrate [5]. In the present paper, investigates us ZnO films were deposited under different annealing temperatures on glass substrates via CBD bath, the paper explains how raising the annealing influence on the optical films properties compared to the results among them, this method is useful for making thin films.

2. Experimental method

2.1. Preparation of samples

Glass substrate as one form (objekttrager) has been used to prepare ZnO films by (CBD) process, after boiling (15 min) in distilled$\mathrm{H_2O}$, the substrate was then soaked in acetone and alcohol for (15 min) and washed using distilled$\mathrm{H_2O}$ to rinsing. After that, the substrates are

---

[*] Corresponding author: sabahibab@gmail.com

weighed after cleaning with a sensitive balance Mittler type with sensitivity $10^{-4} mg$, and using material of zinc nitrate ($\mathrm{Zn(NO_3)_2.6H_2O}$), purity (99.99%) and supplied by (Fulki) it is a white solid with a rapid solubility in water and a molecular weight of (297.51 gm/mol). Prepare a zinc nitrate solution with a concentration of 0.3M by gradually dissolving the required weight of the material in 300ml distilled water using magnetic stirrer (700Hz) about (15min) so we get a clear, homogeneous, colorless solution. After the dissolution process is completed and the appropriate solution is obtained, the gradual addition (distillation) of aqueous ammonia (NH_4OH) with continuous stirring then the color of the solution changes to a milky color, after that continue adding the ammonia solution until we get a clear, homogeneous, colorless solution again. The PH of the solution was measured using digital (PH meter) type (Inolab PH720), and it ranged from (9-10.5). The cleaned glass substrates are immersed (at room temperature) vertically in the solution without magnetic stirring for (30min), solid ZnO particles may be formed in aqueous solution after we raise the temperature to 80℃ for (3-4) hours. After that the heat was turned off and the samples were kept inside the baker containing the solution, and it was taken out after about one day. Fig. (1) Shows the precipitation system that was utilized ZnO films for preparation.

Fig. 1. Chemical bath deposition method.

The mechanism of reaction is shown during this process in Equations (1)-(4) [6].

$$H_2O + NH_3 \rightarrow OH^- \tag{1}$$

$$Zn^{2+} + 4NH_3 \rightarrow Zn(NH_3)_4^{2+} \tag{2}$$

$$Zn(NH_3)_4^{2+} + OH^- \rightarrow Zn(OH)_2 + (NH_3)_4 \tag{3}$$

$$Zn(OH)_2 \rightarrow ZnO + H_2O \tag{4}$$

2.2. Characterization of CBD-ZnO thin films:

Diffraction of X-ray (XRD) along radiation of Cu K_α possessing 1.5406Å as λ, the 2θ around (20° to70°) be applied on prepared thin films to assured the crystal structure. While the optical transmission and absorbance of as-deposited film and annealed at different temperatures (373, 473, 573) K of CBD-ZnO thin films were studied utilizing SP-3000NANO optima (UV-V is spectrophotometer) in the (300 -1000) nm λ area.

3. Results and discussion

3.1. Structural analysis

Fig. 2 illustrates pattern of XRD for samples were annealed at temperatures (373, 473 and 573) K to know the annealing procedure effect on the structural ZnO films properties. Also, the same figure shows that the non-annealing sample has amorphous structure and no peak has grown on it, which indicates the loss of crystallization of the ZnO thin film. Peaks appear when annealing samples at different temperatures for 1h, and more peaks are growing at annealing temperature 573K. Peaks diffraction at angles $(31.74^{\circ}, 34.3^{\circ}, 36.04^{\circ}, 47.32^{\circ}\ and\ 56.48^{\circ})$ congruenting to planes (100), (002),(101),(102) and (110)) respectively. Designated peaks indicate to the formation of polycrystalline with hexagonal wurtzite structure of zinc oxide and grows along (101) plane, in good agreement to the peaks of standard ZnO structure (JCPDS 00-036-1451). The lattice constant of ZnO films ($a = 2.87$ Å, $\mathrm{c} = 4.93$Å were measured by the following equations [7]:

$$a = \sqrt{\frac{1}{3}}\frac{\lambda}{\sin\theta} \tag{5}$$

$$c = \frac{\lambda}{\sin\theta} \tag{6}$$

The c-axis ZnO films orientation which greatly depends on concentration of initial Zn and films were oriented preferentially at c-axis [8]. Crystallite size along the preferentially oriented crystal plane (101) of thin films ZnO was detected by Debye Scherer formula [9]:

$$D = \frac{k\lambda}{\beta\cos\theta} \tag{7}$$

where D is the crystallite average size, ($\lambda = 1.5406$ Å) is the X-ray λ, k is Scherer's constant, β is the broadening of the peak at FWHM (half maximum full width) and θ is the diffraction angle for each peak. The (FWHM) value of the diffraction peak (101) and is equal (0.26°), which demonstrates the best crystalline quality for prepared films. Half maximum full width is decrease when zinc plane concentration increases (101). The crystalline quality gets better of the zinc oxide films when the concentration of zinc becomes high. In order to calculate the density of dislocation (δ), the dislocation lines length /unit crystal volume can be specified, which can be written in the following formula below [10]:

$$\delta = \frac{1}{D_{av}^{2}} \tag{8}$$

The strain (ε) of the thin films ZnO and the stress (σ) might be determined by means of the following equations [11]:

$$\varepsilon = \frac{\beta\cos\theta}{4} \tag{9}$$

$$\sigma = -232.8 \times \varepsilon \tag{10}$$

Table 1 displays the determined values of the ZnO structural parameters (Crystallite thickness, dislocation density, strain and stress). The negative sign of the stress value means there is a compressive stress on the ZnO films. The larger stress value for the films prepared at 473K, and decreases with increased the annealing temperature. The density of dislocation and strain ZnO films values decrease with annealing temperature increasing and then begin to increase at temperature 300°C. This behavior of the films indicates that the annealing temperature reduces lattice defects and elevates the crystalline via atoms rearranging in lattice of crystalline [12, 13].

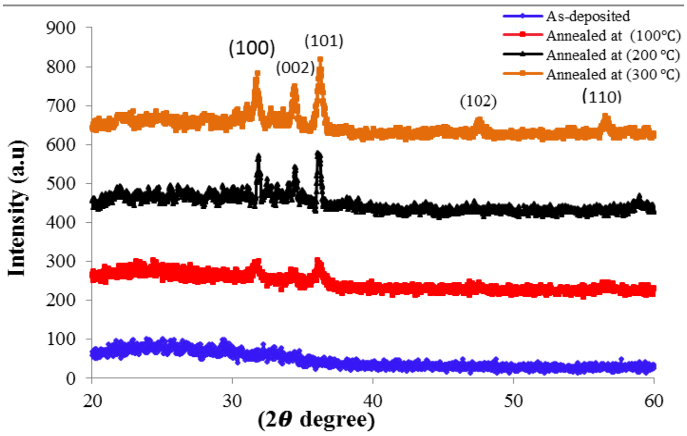

Fig. 2. X-ray ZnO thin films diffraction at various annealing temperature.

Table 1. X-ray ZnO thin films diffraction parameters for plane films (101).

Samples	**SIze of crystallite D (nm)**	**Density of dislocation $\delta \times 10^{-3}$ (lines nm^{-2})**	**Strain, ε (%)**	**Stress (GPa)**
As -prepared	Amorphous			
Annealed at 100 ℃	15.04291	0.004421	0.119027	-27.70949
Annealed at 200°C	20.66658968	0.0023414	0.076467	-17.6928
Annealed at 300°C	15.80357	0.004006	0.111806	-26.0494

3.2. Optical properties

3.2.1. The transmittance and absorbance

Fig. 3 illustrates the optical transmittance and absorption spectra as λ function for CBD-ZnO as-deposited thin films and annealing at different temperatures (373, 473, 573) K. Absorbance spectra of CBD-ZnO thin films exhibits strong absorbance below 340nm which indicates that the film has wide transparency throughout the visible region, confirming the ZnO thin films crystallinity. This result is good agreement with the research [14]. And, Fig. (3a) the as-deposited ZnO films show 83% of the transmittance and the annealed films increase the transmittance values of about 86% and 89% of the annealed films at 373K and 473K respectively, when the temperature of the annealing increases, the thin films stoichiometry increases, i.e. the defects number decreases. The light loss due to the dispersion of defects centers decrease results in the increase of the transmittance [13, 15, 16]. While the film has low transparency as annealed at 573K because thermal induced defects increase dramatically, ZnO film generates low quality [17].

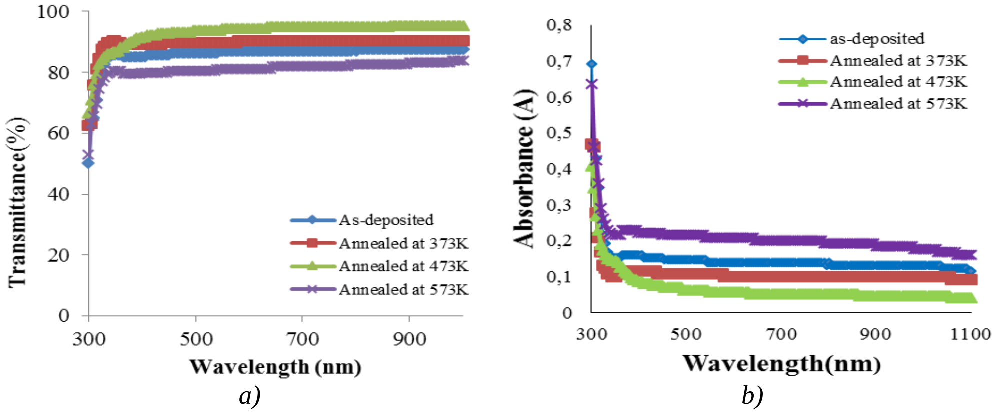

Fig. 3. λ dependence on CBD-ZnO films (a) transmittance and (b) absorbance spectra.

3.2.2. The Coefficient of Absorption

As for the absorbance (A) and the thickness (t) of ZnO films (about 100nm was determined using gravimetric method) the absorption coefficient (α) was estimated from equations [14]:

$$\alpha = 2.303\frac{A}{t} \tag{11}$$

$$A = log\frac{1}{T} \tag{12}$$

Fig. 4 shows the coefficient of absorption (α) decline in photon energy law due to electrical transfer probability between conduction and valence bands is so low and the absorption coefficient will gradually elevate to high energy ($h\upsilon > E_g$) for all samples [18], as the temperature of the annealing increases, the absorption edge changes at blue shift (i.e. shifts to short λs).

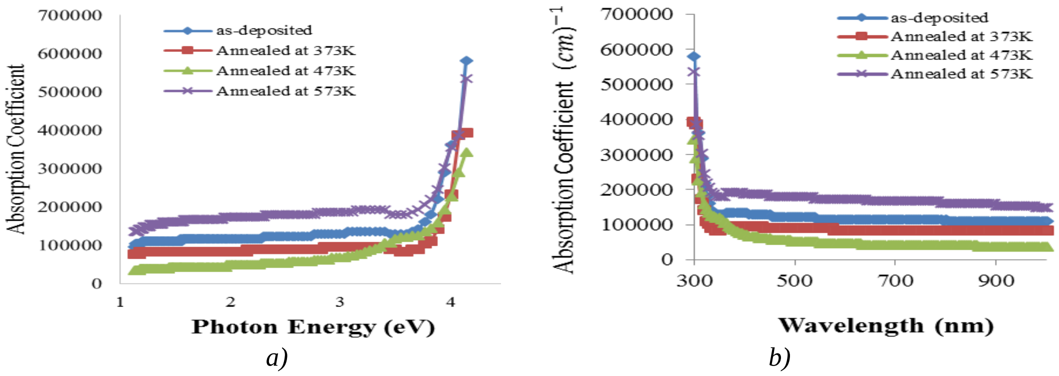

Fig. 4. Coefficient of optical absorption of the CBD-ZnO films as photon energy and λ function.

3.2.3. Optical Band Gap

The equation relates the optical energy gap (E_g) and the absorption coefficient (α) is [14]:

$$\alpha = \left(\frac{k}{hv}\right)\left(hv - E_g\right)^{\beta} \tag{13}$$

Since k= a constant, h = constant of Planck's, hv= photon energy incident and β is a number that describes electronic transition essence between conduction and valence bands. For transitions directly permitted $\beta = 1/2$ and a direct bandgap semiconductor is considered as ZnO. Hence the formula employed is:

$$\alpha = \left(\frac{k}{h\nu}\right)\left(h\nu - E_g\right)^{1/2} \tag{14}$$

$$\text{Which gives } (h\nu\alpha)^2 = C\left(h\nu - E_g\right) \tag{15}$$

Since C is constant. The $(h\nu\alpha)^2$ variance vs. $h\nu$, as gained by formula (15) is illustrated at Fig. 5 as-deposited and annealed CBD-ZnO at various temperatures; The sample $E_g$energy gap was calculated for various annealing temperature where $h\nu$ at the X-axis from every curve linear intercept. Table (2) provides the filmsE_g values deposited at various annealing temperatures. As can be seen from Table (2), the optical gap band energy for CBD-ZnO deposited thin films is 3.75eV and increase to 3.77eV and 3.78 eV by annealing at 373and 473K, respectively, while E_g decrease to 3.73eV for the film annealed at 573K. By Fig. (5) The edge optical absorption shows a little blue shift by increasing temperature of annealing to 373 and 473K. Nonetheless, after the annealing temperature at 573K it shows visible red shift, the optical edge absorption shifts might be because ZnO film consistency changes along an increase in temperatures of annealing. The ZnO absorption edge blue shift is associated typically with enhanced thin film stoichiometry (i.e. the number of defect decreases)[17]. While optical absorption edge redshift increases dramatically with temperature annealing at 573K due to the thermal induced defects, ZnO film generated in low quality. This bandgap energy behavior with annealing temperature is on line with other studies; i.e., A. Khayatian et al. [19] who observed optical ZnO nanorods band gap was grown using method of simple 2-step chemical deposition bath and was found to be (3.1, 3.2 and 2.9)eV at temperature of 300℃, 400℃ and 500℃ for 2 durations of time (1 and 5h), respectively, the reason for this is that the declined band gap in semiconductor films being non-styochiometric oxide caused via the sub-oxide stated correlated with the vacancies of oxygen. Sendi and Mahmud [20] have reported and improvement in the energy bandgap of (3.392, 3.396 and 3.397) eV for (as-grown, 450℃ and 550℃), respectively. Then quantum size reduction influence (or energy gap band) of (3.363, 3.358 and 3.353)eV for (650℃, 750℃ and 850℃) of the ZnO nanostructures, respectively, they interpret this as a heavy desorption of surface oxygen molecules whereas the decreased value of this ZnO band gap is due to an increase in the sample tensile stress. Thus S. W. Xue et al.[17] observed an increase of almost 10meV in band gap energy to temperature of annealing up to 750℃ and a decline of about 10meV at temperatures of annealing between (750-950)℃. They attribute the optical ZnO films absorption edge blue shift increasing due to crystallization quality. Some researchers have explained that lower band gap energy after annealing may result from the oxygen loss from the surface, so that the material at the annealing temperatures may become relatively more O-rich [21]. Fig. 6 Illustration the band gap energy variation as different temperature of annealing function on films of ZnO.

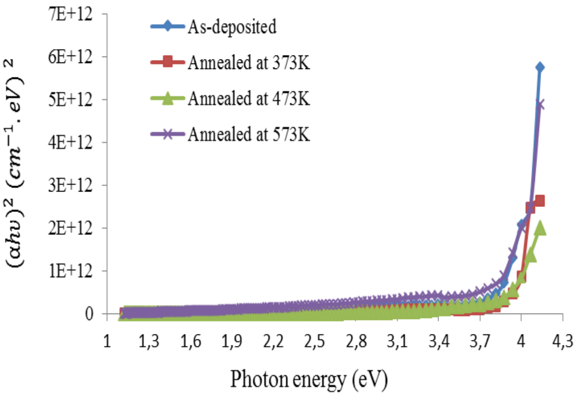

Fig. 5. Variation of band gap for as CBD-ZnO annealed and deposited thin films at various temperatures of annealing.

Table 2. Energy gap values (E_g) ZnO thin films at various temperatures of annealing.

CBD-ZnO Thin films	As-deposited	At 373K	At 473K	At 573K
$E_g(eV)$	3.75	3.77	3.78	3.73

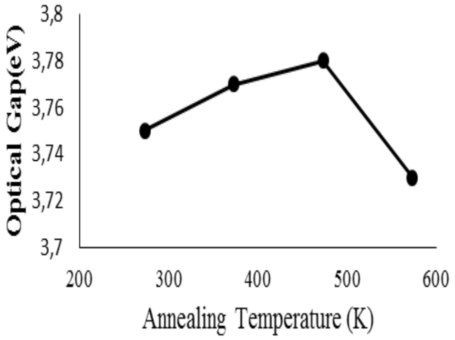

Fig. 6. Illustration of bandgap energy variance as a function of the different temperature of annealing on films of ZnO.

4. Conclusions

Thin films of ZnO deposited via method of CBD was annealed at various temperatures (373, 473 and 573) K at 1h. Patterns of XRD illustrate that crystallization thin films of ZnO was improving due to treatment of annealing and changes in samples characters because of annealing temperature changes and layers structure. The optical properties of the ZnO film have been studied, with each optical transmittance spectra and energy band gap increasing at (373K and 473K) but decreasing at 573K. The optical band gap red-shift and blue-shift of film are associated by improving and degrading ZnO film quality, respectively. Finally, the treatment with annealing plays significant role to control properties as structural and optical.

References

[1] M. Karunakaran, R. Chandramohan, S. Gomathi, K. Radhi Devi, S. Balamurali, T. Mahalingam, International journal of pharmaceutical and chemical sciences **2**(4), (2013).

[2] Albert C. Aragones, A. Palacios-Padros, F. Caballero-Briones, Fausto Snaz, Electrochimica acta **109**, 117- (2013).

[3] Yasemin Pepe, Mehmet Ali Yildirim, Ahmet Karataya, Aytunc Ates, Huseyin Unver, Ayhan Elmali, Optical Materials (2019).

[4] Naceur Selmane, Ali Cheknane, Nourddine Gabouze, Nabila Maloufi, Michel Aillerie, E3S Web of Conferences **22**, 00155 (2017).

[5] E. Pourshaban, H. Abdizadeha, M. R. Golobostanfard, 5th International Biennial Conference on Ultrafine Grained and Nanostructured Materials, UFGNSM15, Procedia Materials Science **11**, (2015).

[6] Shahin K. Shaikh, Sumayya I. Inamdar, Vinayak V. Ganbavle, Kesu Y. Rajpure, Journal of Alloys and Compounds **664**(15), 242 (2016).

[7] Y. Ammaih, A. Lfakir, B. Hartiti, A. Ridah P. Thevenin, M. Siadat, Opt. Quant. Electron. **46**, 229 (2014).

[8] F. K. Konan, B. Hartiti, H. J. Tchognia Nkuissi, A. Boko, Journal of Materials and Environments Sciences **10**(10), 1003 (2019).

[9] T. O. Berestok, D. I.kurbatov, N. M. Opanasyuk, A. D. Pogrebnjak, O. P. Manzhos, S. M. Danilchenko, Journal of Nano-and Electronic Physics **5**(1), 1 (2013).

[10] M. Saleem, L. Fang, H. B. Ruan, F. Wu, Q. L. Huang, C. L. Xu, Y. Kong, International Journal of Physical Sciences **7**(23), 2971 (2012).
[11] M. H. Kabir, M. M. Ali, M. Abdul Kaiyum, M. S. Rahman, Journal of Physics Communications **3**(10), (2019).
[12] Geum Ran Yi, Han Sol Kim, Do Hyung Lee, Bada Kim, Chang Kyo Kim, Molecular Crystals and Liquid Crystals **678**(1), 43 (2019).
[13] Mohsin Ghasemi Varnamkhasti, Hamid Reza Fallah, Mehdi Zadsar, Vacuum **86**, 871 (2012).
[14] Yenpei Fu, Jianjhih Chen, Key Engineering Materials **602-603**, 871 (2014).
[15] N. J. Egwunyenga, L. N. Ezenwaka, I. A. Ezenwa, N. L. Okoli, Materials Research Express **6**(10), (2019).
[16] R. Chandramohan et al., Materials science and engineering B **176**, 152 (2011).
[17] S. W. Xue et al., Journal of alloys and compounds **448**, 21 (2008).
[18] R. A. Al-Wardy, IOP Conf. Series: Journal of Physics: Conf. Series **1032**, 012002 (2018).
[19] A. Khayatian et al., Int. j. light electron opt. (2016).
[20] Rabab Khalid Sendi, Shahrom Mahmud, Journal of Physical Science **24**(1), 1 (2013).
[21] Wen-Yao Huang, Tung-Li Hsieh, Ann-Kuo Chu, Journal of information engineering and Applications **2**(5), (2012).